

Functional adaptation underpinned the evolutionary assembly of the earliest vertebrate skeleton

Duncan J. E. Murdock,*¹ Emily J. Rayfield, and Philip C. J. Donoghue*

School of Earth Sciences, University of Bristol, Life Sciences Building, 24 Tyndall Avenue, Bristol BS8 1TQ, UK

*Authors for correspondence (e-mail: duncan.murdock@le.ac.uk; phil.donoghue@bristol.ac.uk)

¹Present address: Department of Geology, University of Leicester, University Road, Leicester LE1 7RH, UK

SUMMARY Conodonts are the first vertebrates to bear a mineralized skeleton, restricted to an array of tooth-like feeding elements. The functional implications for the development of tooth-like elements differentiated into two tissues is tested using 2D finite element modeling, mapping the patterns of stress and strain that elements with differing material properties exhibited during function. Addition of a stiff crown does not change the patterns of stress, rather it reduces the deformation of the element under the same force regime, and distributes stress more evenly across the element. The euconodont crown, like vertebrate dental enamel, serves to

stiffen the element and protect the underlying dentine. Stiffness of the crown may be a contributing factor to the subsequent diversity of euconodont form, and logically function, by allowing a greater range of feeding strategies to be employed. The euconodont crown also serves as an analogue to enamel and enameloid, demonstrating that enamel-like tissues have evolved multiple times in independent vertebrate lineages, likely as a response to similar selective pressures. Conodonts can, therefore, serve as an independent test on hypotheses of the effect of ecology on the development of the vertebrate skeleton.

INTRODUCTION

Conodonts are an extinct group of eel-like jawless vertebrates, the earliest known members of the gnathostome lineage (Donoghue et al. 2000), and bear the earliest manifestation of a mineralized skeleton in vertebrates. The conodont mineralized skeleton constitutes an oral/pharyngeal array of dental elements, each comprised of a dentine-like core capped by an enamel-like crown (Donoghue 1998). Indeed, conodont dental elements have long been interpreted as the earliest instance of the “odontode” skeletal patterning unit that characterizes the teeth and scales of total-group gnathostomes (Donoghue 1998), inspiring the hypothesis that teeth evolved before, and perhaps even independently of dermal scales (Smith and Coates 1998). However, despite the structural, topological and developmental similarities between conodont and gnathostome skeletal tissues (Donoghue and Aldridge 2001), it has been shown that these tissues, indeed, this dental organogenic module, evolved entirely independently, in parallel within the conodont and gnathostome evolutionary lineages (Fig. 1; Murdock et al. 2013; Donoghue and Rücklin 2014). Thus, though conodonts may not be integral to the evolutionary origin of the skeleton inherited by living jawed vertebrates, they constitute a remarkable natural experiment in the evolution of a dental organogenic module, which precisely parallels that of their sister, gnathostome, lineage. It has been argued that odontode structure was achieved independently in the oral and dermal skeletons of gnathostomes, through the parallel

cooption of the same gene regulatory network (Fraser et al. 2010). However, the independent evolution of a common dental structure in conodont and gnathostomes suggests that the proximal cause is functional, rather than developmental. Conodonts, thus, are a unique resource in which to test this hypothesis since, though there is evidence for the independent recruitment of enamel-like tissues to teeth in distinct lineages of gnathostomes (Donoghue 2001), the gradual evolutionary assembly of euconodont dental elements is well documented in the fossil record (Murdock et al. 2013). Thus, in exploring the functional context of the evolutionary assembly of the canonical suite of enamel- and dentine-like dental tissues that characterize the euconodont dental organogenic module, we aim to obtain general insights that are relevant to understanding the evolutionary origin of this model organogenic system in gnathostomes.

Euconodonts, which comprise the bulk of the diversity and longevity of the conodont evolutionary lineage, are distinguished structurally from their paraphyletic paraconodont relatives whose dental elements are comprised solely of dentine-like tissues (Murdock et al. 2013). We generated submicron resolution digital images of paraconodont and euconodont dental elements, from which we derived digital mesh models that were subjected to finite element analyses (FEA) that simulated implied dental loads. Paraconodont and euconodont elements vary both in terms of structure and morphology. Therefore, to control for variation in morphology we contrasted the patterns of stress and strain experienced by

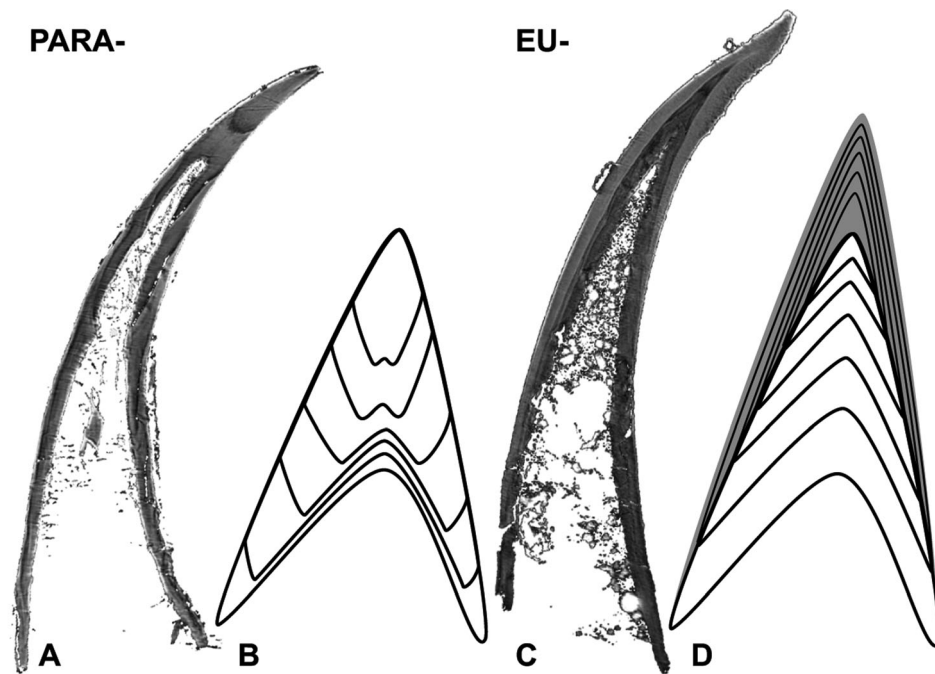


Fig. 1. Comparison of the histology of elements of the paraconodont *Prooneotodus* sp. (A and B) and the euconodont *Proconodontus posterocostatus* (C and D). SRXTM generated longitudinal cross-sections (A and C) and generalized schematic drawings (B and D). Paraconodont elements consist of a single tissue type characterized by punctuated incremental growth lines, which define hollow conical laminae. Euconodont elements consist of two tissues: the basal body (white), with the same pattern of growth as a paraconodont element; and, the crown (gray).

materially homogenous finite element (FE) models of morphologically similar euconodont and paraconodont elements, that is, all elements attributed a paraconodont-like structure consisting of single tissue. We contrasted these results with patterns of stress and strain experienced by structurally differentiated FE models of euconodont elements consisting of two tissues.

The results of our analyses demonstrate that applied dental stresses are distributed more effectively in euconodont versus paraconodont structural grades. Thus, as well as facilitating greater morphological differentiation of the functional surface of elements through ontogeny, our FE analyses indicate that the euconodont crown served to diminish stress during functional loading. These results may explain the competitive displacement of paraconodonts by the euconodonts, as well as the convergent evolution of dental structure seen also in the earliest jawed vertebrates. Evidently, similarities in the dental structure of conodonts and gnathostomes appear to be a consequence of functional convergence and the selective advantage of reducing stress imposed by functional loading through the evolution of a stiff hypermineralized enamel-like capping tissue.

MATERIALS AND METHODS

We compared morphologically similar well-preserved elements of paraconodont and euconodont species from a range of Middle

Cambrian to Lower Ordovician deposits, based on their overall similarity in morphology, and representative nature of typical forms for each group. Paraconodonts: TC1115, *Furnishina* sp. from Threadgill Creek section, Wilberns Formation, central Texas, 1115 feet above base of Cambrian strata (see Miller 1980 for further details); and, Smithsonian National Museum of Natural History (USNM) 593438, *Prooneotodus* sp., from the *Cambroostodus* subzone of the *Eoconodontus* zone of the Windfall Formation, Upper Cambrian, Eureka County, Nevada, USA. Euconodonts: USNM 593440 *Proconodontus serratus* also from the Windfall Formation; and, Lapworth Museum of Geology BU4421, *Proconodontus posterocostatus* from Gros Ventre Formation, Late Cambrian, Bighorn Mountains, Wyoming, USA. Specimens were mounted on 3 mm brass stubs using clear nail varnish and volumetrically characterized using synchrotron radiation X-ray tomographic microscopy (SRXTM) (Donoghue et al. 2006) at the X02DA TOMCAT beamline (Stampanoni et al. 2006) at the Swiss Light Source, Paul Scherrer Institut, Villigen, Switzerland. Measurements were taken using 10× and 20× objective lenses at 10–15 keV. For each dataset, 1501 projections over 180° were acquired, resulting in volumetric data with voxel sizes of 0.74 and 0.36 μm, respectively.

Functional analysis was undertaken using a 2D FE approach. A two dimensional FE-mesh of each element was created from a longitudinal section standardly oriented to bisect the distal tip

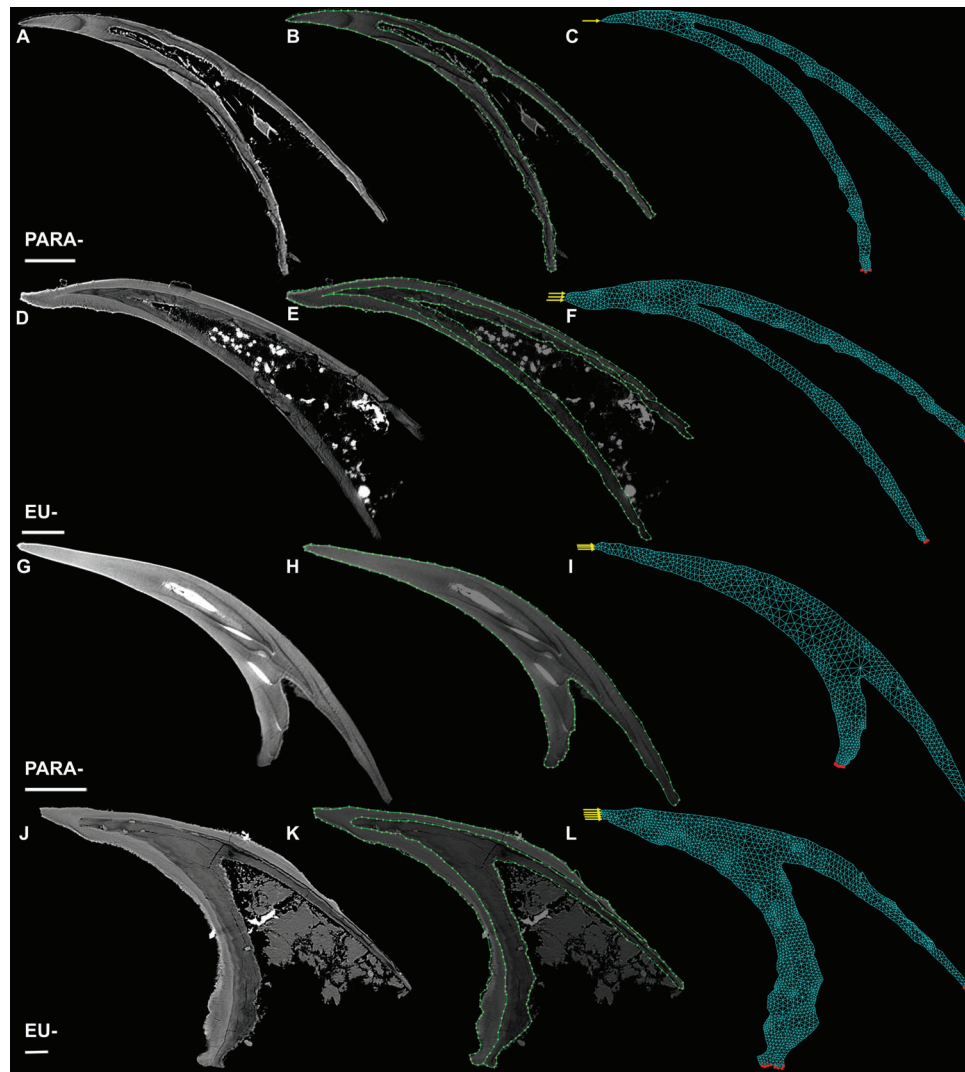


Fig. 2. SRXTM generated longitudinal cross-sections (A, D, G, and J) with points and curves delimiting the outer and inner surface and the crown-basal body (enamel-dentine) junction (B, E, H, and K), and finite element mesh (C, F, I, and L) for elements of *Prooneotodus* sp. (A–C), *Proconodontus posterocostatus* (D–F), *Furnishina* sp. (G–I) and *Proconodontus serratus* (J–L). Nodes constrained during analysis are highlighted with squares, and those to which a load was applied are indicated with arrows parallel to the direction in which the load was applied. Scale bars = 50 μm .

and basal cavity. Considering the elements examined are essentially conical, a 2D longitudinal section is representative of the majority of the element morphology. These were generated by taking an oblique slice through the 3D volume of each complete specimen generated from the tomographic data. Outline x, y coordinates were imported into the Geostar geometry creator component of the COSMOSM (Dassault Systèmes Solidworks Corp., Concord, MA, USA), and “meshed” to produce an interconnected grid of three-noded triangular FEs representing a standardized longitudinal cross-section through each element. The meshes contained the following number of elements: *Prooneotodus* sp., 1388; *P. posterocostatus*, 1788; *Furnishina* sp., 1284; *P. serratus*,

2788. The models were constrained to six degrees of freedom over the minimum number of nodes at the proximal margin, making sure to constrain both crown and basal body in the euconodonts, this resulted in the following number of nodes constrained: *Prooneotodus* sp., 6; *P. posterocostatus* 6; *Furnishina* sp. 8; *P. serratus* 13 (Fig. 2). The surface area was measured from each cross section and a force scaled to the surface area and relative to the smallest element (*Prooneotodus*) was divided equally over the distal most nodes of each element: *Prooneotodus* sp., 1 N applied to one node; *P. posterocostatus*, 0.6 N applied to three nodes (1.8 N total); *Furnishina*, 0.34 N applied to three nodes (1.02 N total); *P. serratus* 1.846 N applied to five nodes (9.23 N total). This process generated an applied force that

was proportional to the surface area dimensions of each model. The force was applied in the x-direction, orientated down the long axis of each element from distal to proximal, to simulate loading at the distal-most part of the cusps (consistent with models of conodont element function). This approach tests the performance of each conodont shape, irrespective of differences in size (Dumont et al. 2009).

The material properties of the teeth of the bonnethead shark (*Sphyrna tiburo*) (Whitenack et al. 2010) were assigned to conodont elements. The Young's modulus attributed to the models was the mean value taken to three significant figures, that is, 68.8 GPa for enameloid and 22.5 GPa for orthodentine, and each tissue was treated as isotropic and homogenous. Preliminary analysis with approximated values for Young's modulus (70 and 20 GPa, respectively) showed that minor fluctuations in Young's modulus had no significant effect on the pattern of results, providing the crown remained two to three times stiffer than the basal body. Both crown and basal body were treated as linearly elastic with a Poisson's ratio (the negative ratio of transverse to axial strain) of 0.3, which is a reasonable estimation and typical of biological apatite (Waters 1980). These data were selected because of the relative phylogenetic proximity of sharks and conodonts, in comparison to alternative sources of material property data (and the impossibility of obtaining such data from extinct taxa). Furthermore, shark orthodentine is structurally and histologically analogous to the euconodont basal body (Sansom et al. 1992). The material properties of euconodont crown tissue are more problematic; euconodont crown tissue and vertebrate enamel are not homologous but they are structurally analogous. There is little consensus on the precise properties of vertebrate enamel, not least because it may have multiple origins (Donoghue 2001) and is strongly anisotropic (Spears 1997). However, the Young's modulus for *S. tiburo* enameloid is congruent with the majority of observed data for vertebrate enamel (Jones et al. 2012).

The affect of morphological diversity on functional differentiation was tested by comparing patterns of stress experienced in paraconodont and euconodont element models during simulated loading. Stress is a measure of force per unit area, and gives some indication of the likely points of fracture or weakness in the structure. In addition, an overall pattern of less stress can be used to infer a superior ability to successfully function under greater loading conditions without damage to the structure. However, this does not take into account the fundamental difference between paraconodont and euconodont elements, that is, the presence of a stiff outer layer—crown tissue. The affect of structural differentiation on functional differentiation was explored by (i) comparing patterns of strain between paraconodont and euconodont elements that showed similar patterns of stress in the first experiments and, (ii) by comparing patterns of strain in euconodont elements modeled as two differentiated tissues with different material properties, to models where the entire element possessed the material properties of the basal

body alone. Strain, a measure of deformation, is used as it is a function of both the morphology of the structure and the material properties it exhibits. We focus on maximum and minimum principal stresses (E_{\max} and E_{\min}) that typically indicate tensile stresses and compressive stresses, and equivalent strain, that illustrates the distribution of high tensile and compressive strains.

RESULTS

Morphological variation and function

All of the models show that when a force is applied to the distal tip of both eu- and paraconodont elements, most of the stresses are confined to the outer margins of the element (Fig. 3). There is a concentration of tensile stress (hot colors) at the distal-most part of the basal cavity, associated with deformation of this region. High compressive stresses (cool colors) are found on the outer surface of the cusp and the proximal surface of the basal cavity. Exceptional stress values at the extreme proximal margins are an artefact of constraining the model at these nodes.

In *Prooneotodus*, significant compressive stresses (Fig. 3B), and shear stresses (Fig. 3C), are experienced on the outer margins surrounding the top of the basal cavity, and significant tensile stresses at the apex of the inner margin of the basal cavity (Fig. 3A). During simulated function, the tip of the cusp is displaced laterally but most of the deformation occurs in the walls surrounding the basal cavity (Fig. 3E).

The element of the euconodont *P. posterocostatus* bears a similar pattern of stresses, with compressive stresses (Fig. 3G) and shear stresses (Fig. 3H) concentrated on the outer margins of the distal basal cavity and tensile stresses at the inner margin (Fig. 3F). Similarly, although displaced, the tip of the cusp remains relatively undeformed while considerable deformation is evident around the basal cavity (Fig. 3J).

By contrast, in *Furnishina*, stress is distributed evenly on the margins of the element (Fig. 3, K–M), with lower maximum values than those seen in either *Prooneotodus* or *P. posterocostatus*. The parts of the element proximal to the basal body experience virtually no deformation while the distal tip of the cusp is deflected and compressed parallel to the direction in which the load is applied (Fig. 3O).

The element of *P. serratus* shows a similar pattern to that of *Furnishina* but with an asymmetry across the element. The thinner, outer part of the cusp experiences significantly higher compressive and shear stresses than the inner part (Fig. 3, P–R). The inner, thicker, part of the cusp also shows very little deformation compared to the rest of the element (Fig. 3T).

Structural differentiation and function

Euconodont elements with a relatively deep (*P. serratus*) and shallow (*P. posterocostatus*) basal cavity were compared to

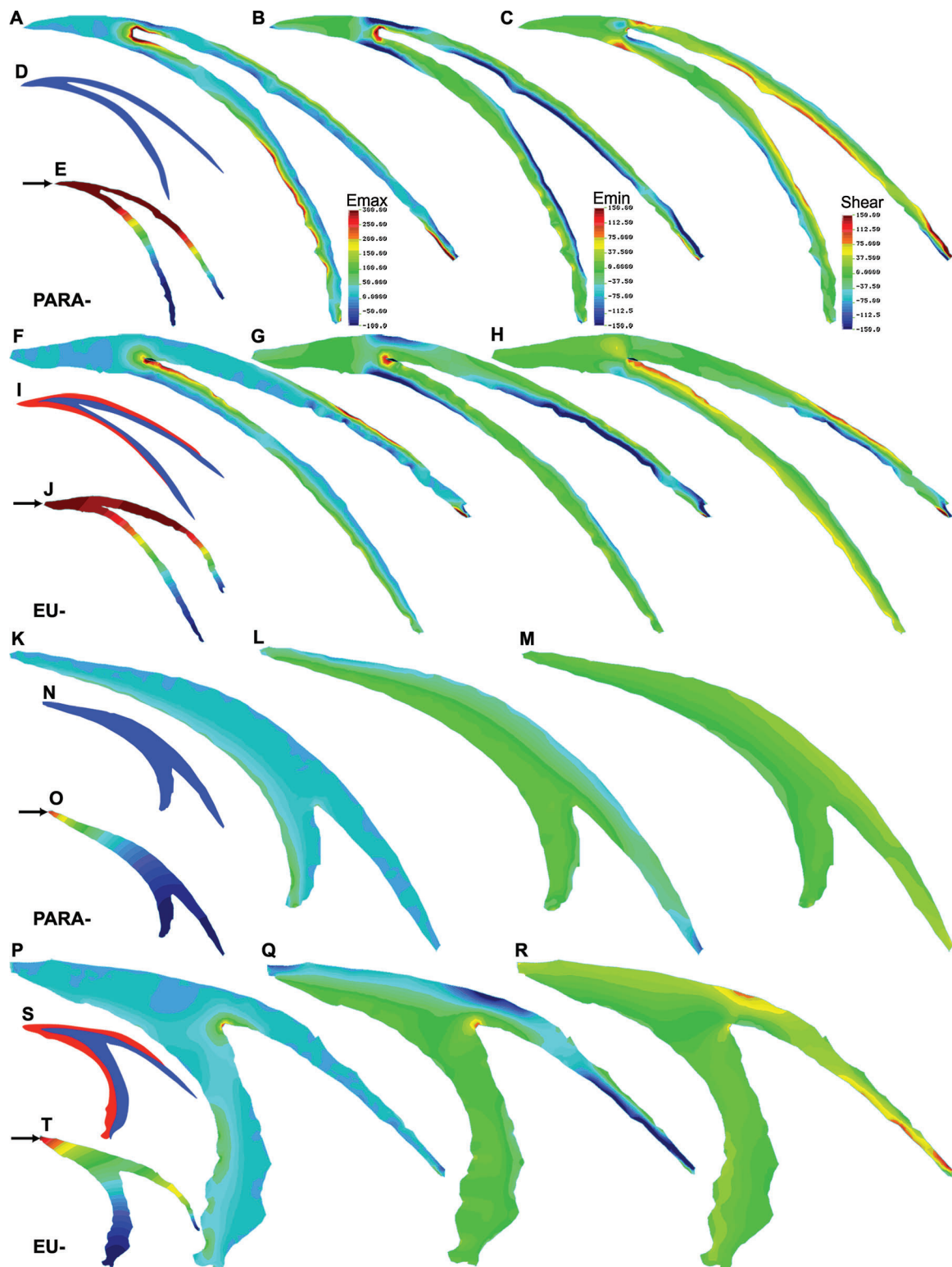


Fig. 3. Patterns of stress and deformation in elements of: paraconodonts, *Prooneotodus* (A–E) and *Furnishina* (K–O); and euconodonts, *Proconodontus posterocostatus* (F–J) and *Proconodontus serratus* (P–T). (A, F, K, and P) Principal stress 1 (E_{\max}), mainly tension, scale inset in (A). Warm colors indicate high tensile stresses, mid-blue indicates little to no stress. (B, G, L, and Q) Principal stress 3 (E_{\min}), mainly compression, scale inset in (B). Cool colors indicate high compressive stresses, green indicates little to no stress. (C, H, M, and R) In-plane shear stress (Shear), scale inset in (C). Reds and blues indicate hotspots of shear stress, green indicates little to no stress. (D, I, N, and S) Distribution of material properties; blue areas have Young's modulus of orthodentine, red areas that of enameloid. (E, J, O, and T) Arrow indicates position and direction of load; plot shows deformation of element, with increasingly warm colors indicating increasing deformation. Units of stress are Pa or Nm^{-2} .

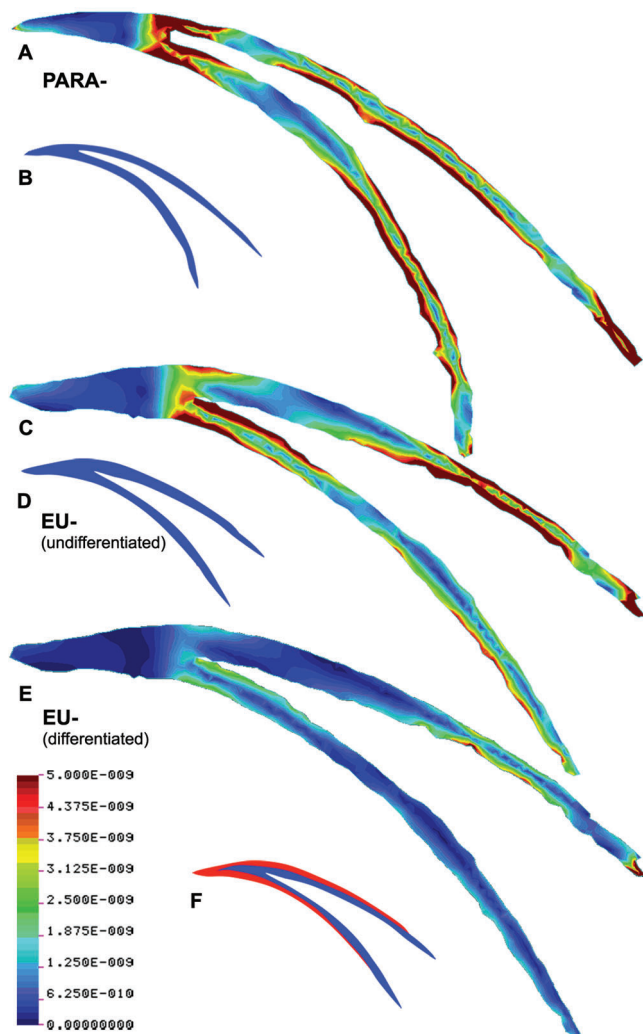


Fig. 4. Patterns of equivalent strain in elements of *Prooneotodus* (A) and *Proconodontus posterocostatus* (C and E) with inset to show the distribution of material properties in each model (B, D, and F); blue areas have Young's modulus of orthodentine, red areas that of enameloid. Warm colors indicate regions of high strain. Paraconodont and undifferentiated euconodont elements show very similar magnitude and distribution of strain, but the strain experienced is greatly reduced with the addition of a stiff crown (E).

paraconodont counterparts, both as differentiated and undifferentiated models. The elements of *Prooneotodus* sp. (Fig. 4A) and *P. posterocostatus* (Fig. 4, C and E) show strain concentrated in three parts of the elements: (i) the distal-most tip of the cusp where the load is applied, (ii) the distal-most margin of the basal body, and (iii) the lateral margins of the basal body. The pattern of strain is effectively the same across all three models, however, in the differentiated model of *P. posterocostatus* the maximum values of strain are markedly reduced.

The elements of *Furnishina* sp. (Fig. 5A) and *P. serratus* (Fig. 5, C and E) bear most of the strain along the outer margin of

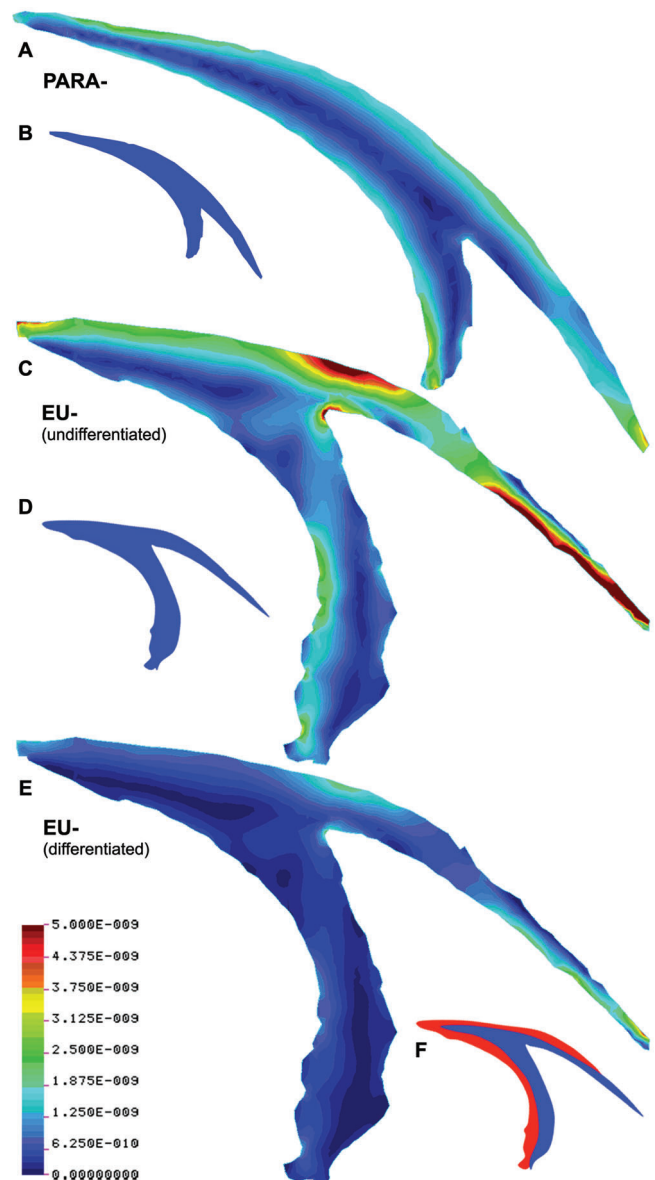


Fig. 5. Patterns of equivalent strain in elements of *Furnishina* (A) and *Proconodontus serratus* (C and E) with inset to show the distribution of material properties in each model (B, D, and F); blue areas have Young's modulus of orthodentine, red areas that of enameloid. Paraconodont and undifferentiated euconodont elements show very similar magnitude and distribution of strain except where the element wall thickness is significantly reduced. Also the strain experienced is greatly reduced with the addition of a stiff crown (E).

the elements. The pattern and magnitude of the strain in models of *Furnishina* and the undifferentiated *P. serratus* differ only where the thickness of the wall around the basal cavity is reduced in *P. serratus* (exhibiting higher values of strain than those of *Furnishina*), otherwise they are very closely comparable. The differentiated model of *P. serratus* has this same pattern of strain but, again, with markedly reduced maximum values (Fig. 5E).

DISCUSSION

The results of these experiments demonstrate that the functional performance of conodont elements is influenced principally by differences in morphology and structure. Our FE models based simply on shape and not structure or material composition allow us to isolate the impact of shape variation in exploring the functional performance of paraconodont versus euconodont elements. The principal factor of shape variation in influencing the accommodation of stress in implied loads is identified as the height of the basal cavity in paraconodont and euconodont elements. Proportionally lower basal cavities, such as those seen in the paraconodont *Furnishina* and the euconodont *P. serratus*, allow stress to be distributed more evenly, and the stiffness of the functional surface reduces the strain experienced under equivalent loads. Deeper basal cavities, such as those seen in elements of the paraconodont *Prooneotodus* and the euconodont *P. posterocostatus*, effect to concentrate implied stress around the apex of the basal cavity, exaggerated by the corresponding reduction in thickness of the cusp around the basal body.

If only shape is considered, the two euconodont elements do not have comparable functional performance. Rather, the model of the paraconodont *Furnishina* is closely comparable to the undifferentiated model of the euconodont *P. serratus* and the model of the paraconodont *Prooneotodus* performs most similarly to the undifferentiated model of the euconodont *P. posterocostatus*. Thus, similarity in cross-sectional profile (i.e., depth of basal cavity and corresponding thickness of the cusp) has a greater influence on the distribution of stress, than has relatedness.

Our analyses attempted to discriminate the influence of structure by comparing the performance of models of (i) paraconodont elements and morphologically similar but structurally differentiated euconodont elements, and (ii) structurally homogenous and structurally differentiated euconodont elements. The results of the analyses demonstrate that the additional stiffness of the crown has an overwhelming impact on the response of euconodont elements to loading when compared to paraconodont elements.

Thus, while theories on the advantage of euconodont versus paraconodont element structure identify (i) abrasion resistance (Szaniawski and Bengtson 1993), (ii) due to the episodic growth mode of euconodont elements, the maintenance of functional morphology in the face of mechanical abrasion and brittle failure (Donoghue and Purnell 1999) and, (iii) the flexibility to modify functional morphology through ontogeny (Donoghue 2001), the increased stiffness of euconodont elements is a more proximal selective factor.

The euconodonts have been demonstrated to have derived from paraconodont ancestors (Murdock et al. 2013), supported by the relative timings of their origins in the fossil record. In fact, the ecological turnover in the conodonts associated with the origin of euconodonts has all the diagnostic characteristics of

competitive replacement (Benton 1996). These include (i) the origin and radiation of euconodonts in the Late Cambrian and Early Ordovician is contemporaneous with the ecological displacement and ultimate decline of the paraconodonts (Zhang and Barnes 2004); (ii) the striking similarity in element morphology between paraconodont elements and the earliest euconodont elements reflecting overlap in feeding ecology (see above); (iii) both groups have a congruent geographical distribution and environment, indeed they are often recovered from the same samples (Müller and Hinz 1991) and, crucially, the dominant group possessed a key apomorphy which afforded them an ecological advantage, the euconodont crown.

Though the stiff crowns of the earliest euconodont elements would have acted to distribute and diminish stress, the deep basal cavities and thin crowns of these elements (e.g., *P. posterocostatus*) would have resulted in high levels of stress still being experienced in the basal body, reminiscent of the ancestral paraconodont condition. However, euconodont phylogeny is characterized by the development of proportionally thicker crowns and proportionally diminishing basal bodies (Donoghue and Aldridge 2001) that would have resulted in the basal body no longer experiencing any notable load-related stress. Stress-reduction in the basal body, due to expansion of the stiff crown layer, may ultimately have been the principal factor permitting the morphological diversity observed in euconodont elements, that likely reflects diversity in feeding ecology.

Ultimately, the pattern of evolution in the organization of conodont elements parallels the evolution of teeth which appear initially to have been comprised solely of dentine and bone in the earliest jawed vertebrates (Rücklin et al. 2012) and to have acquired an enamel or an enamel-like cap only latterly within gnathostome phylogeny and, then, apparently independently in chondrichthyans and osteichthyans (Donoghue 2001). The euconodont crown likely evolved under the same adaptive selection pressures as enamel-like tissues in jawed vertebrates. However, the consequent trends in dental evolution are quite different, with the morphogenesis of euconodont elements limited largely to the enamel-like tissue that was subject to repair and enlargement (Donoghue and Aldridge 2001), while gnathostome teeth remain dominantly composed of a dentine core with comparatively thin enamel or enamel-like cap, subject only to replacement. Nevertheless, the results of our experiments lead us to conclude that the similarity of conodont and gnathostome dental elements may not be as remarkable as they seem but, rather, an inevitable consequence of the impact of the parallel imposition of the same functional selection pressures.

CONCLUSIONS

Following the substantiation of the hypothesis that the skeleton of euconodonts derives from that of paraconodonts, we identify

two key morphological trends in euconodont evolution that would have afforded a functional advantage: (i) the origin and subsequent thickening of a stiff cap of enamel-like crown tissues and (ii) the shallowing and ultimate loss of the basal cavity. The ability to accommodate greater load-induced stress in elements with increasingly shallow basal bodies and thicker, more extensive crowns may have driven the increase in diversity and disparity of euconodont elements. In addition this may have been a factor in the competitive replacement of paraconodonts by euconodonts. Enamel-like tissues have been independently derived in a number of vertebrate lineages, the earliest example of which is the euconodont crown, which likely reflects a response to the same selective pressures. This highlights the close relationship between form and function in vertebrate dentition, and the utility of conodont elements in understanding the effect of ecology on the development of the vertebrate skeleton.

Acknowledgments

The SRXTM experiments were performed on the TOMCAT beamline at the Swiss Light Source, Paul Scherrer Institut (Villigen, Switzerland), funded through a project awarded to P.C.J.D. and S. Bengtson (Stockholm). NERC grant NE/G016623/1 to P.C.J.D., a studentship to DJEM funded by NERC and the Paul Scherrer Institut. Thanks to J.E. Cunningham, D.O. Jones and M. Rücklin for assistance at the beamline.

REFERENCES

- Benton, M. J. 1996. On the nonprevalence of competitive replacement in the evolution of tetrapods. In J. Valentine, D. Jablonski, D. H. Erwin, and J. H. Lipps (eds.), *Evolutionary Paleobiology*. The University of Chicago Press, London, pp. 185–210.
- Donoghue, P. C. J. 1998. Growth and patterning in the conodont skeleton. *Philos. Trans. R. Soc. Lond. Ser. B Biol. Sci.* 353: 633–666.
- Donoghue, P. C. J. 2001. Microstructural variation in conodont enamel is a functional adaptation. *Proc. R. Soc. Lond. Ser. B Biol. Sci.* 268: 1691–1698.
- Donoghue, P. C. J., and Aldridge, R. J. 2001. Origin of a mineralised skeleton. In P. E. Ahlberg (ed.), *Major events in Early Vertebrate Evolution: Palaeontology, Phylogeny, Genetics and Development*. Taylor & Francis, London, pp. 85–105.
- Donoghue, P. C. J., and Purnell, M. A. 1999. Growth, function, and the conodont fossil record. *Geology* 27: 251–254.
- Donoghue, P. C. J., and Rücklin, M. 2014. The ins and outs of the evolutionary origin of teeth. *Evol. Dev.* in press.
- Donoghue, P. C. J., Forey, P. L., and Aldridge, R. J. 2000. Conodont affinity and chordate phylogeny. *Biol. Rev.* 75: 191–251.
- Donoghue, P. C. J., et al. 2006. Synchrotron X-ray tomographic microscopy of fossil embryos. *Nature* 442: 680–683.
- Dumont, E. R., Grosse, I. R., and Slater, G. J. 2009. Requirements for comparing the performance of finite element models of biological structures. *J. Theor. Biol.* 256: 96–103.
- Fraser, G. J., Cerny, R., Soukup, V., Bronner-Fraser, M., and Streelman, J. T. 2010. The odontode explosion: the origin of tooth-like structures in vertebrates. *Bioessays* 32: 808–817.
- Jones, D., Evans, A. R., Siu, K. K. W., Rayfield, E. J., and Donoghue, P. C. J. 2012. The sharpest tools in the box? Quantitative analysis of conodont element functional morphology. *Proc. Biol. Sci.* 279: 2849–2854.
- Miller, J. F. 1980. Taxonomic revisions of some Upper Cambrian and Lower Ordovician conodonts with comments on their evolution. *Univ. Kansas Paleont. Contrib.* 99: 1–44.
- Müller, K. J., and Hinz, I. 1991. Upper Cambrian conodonts from Sweden. *Foss. Strat.* 28: 1–153.
- Murdock, D. J. E., Dong, X.-P., Repetski, J. E., Marone, F., Stampanoni, M., and Donoghue, P. C. J. 2013. The origin of conodonts and of vertebrate mineralized skeletons. *Nature* 502: 546–549.
- Rücklin, M., Donoghue, P. C. J., Johanson, Z., Trinajstić, K., Marone, F., and Stampanoni, M. 2012. Development of teeth and jaws in the earliest jawed vertebrates. *Nature* 491: 748–751.
- Sansom, I. J., Smith, M. P., Armstrong, H. A., and Smith, M. M. 1992. Presence of the earliest vertebrate hard tissues in conodonts. *Science* 256: 1308–1311.
- Smith, M. M., and Coates, M. I. 1998. Evolutionary origins of the vertebrate dentition: phylogenetic patterns and developmental evolution. *Eur. J. Oral Sci.* 106: 482–500.
- Spears, I. R. R. 1997. A three-dimensional finite element model of prismatic enamel: a re-appraisal of the data on the Young's modulus of enamel. *J. Dent. Res.* 76: 1690–1697.
- Stampanoni, M., et al. 2006. Trends in synchrotron-based tomographic imaging: the SLS experience. *Proc. SPIE* 6318: 63180M.
- Szaniawski, H., and Bengtson, S. 1993. Origin of euconodont elements. *J. Paleontol.* 67: 640–666.
- Waters, N. E. 1980. Some mechanical and physical properties of teeth. *Symp. Soc. Exp. Biol.* 34: 99–135.
- Whitenack, L. B., Simkins, D. C. Jr., Motta, P. J., Hirai, M., and Kumar, A. 2010. Young's modulus and hardness of shark tooth biomaterials. *Arch. Oral Biol.* 55: 203–209.
- Zhang, S., and Barnes, C. R. 2004. Late Cambrian and Early Ordovician conodont communities from platform and slope facies, western Newfoundland: a statistical approach. In A. B. Beaudoin and M. J. Head (eds.), *The Palynology and Micropalaeontology of Boundaries*, The Geological Society, London, pp. 47–72.